31st EPS Conference on Plasma Phys. London, 28 June - 2 July 2004 ECA Vol.**28G**, P-2.138 (2004)

Full Wave Analysis of Global Instabilities in Tokamaks

T. Akutsu and A. Fukuyama

Department of Nuclear Engineering, Kyoto University, Kyoto, 606-8501, Japan

Introduction

There have been many attempts to include kinetic effects into the MHD equations to describe macroscopic instabilities. We are developing the numerical code TASK/WA to solve Maxwell's equations using kinetic dielectric tensor in order to systematically include the kinetic effects into the analysis of global instabilities in tokamaks. As a first step, we have derived a dielectric tensor $\overleftrightarrow{\epsilon}$ from the multi-fluid equations, taking the effect of electron inertia, pressure gradient, and parallel current into account, and applied it to the analysis of ideal and resistive modes. We have also formulated a kinetic dielectric tensor by integrating along the particle orbit taking account of the resonant interaction between particles and waves.

Full Wave Analysis

The TASK/WA code solves Maxwell's equations for scalar potential ϕ and vector potential $\boldsymbol{A}$ using a magnetic flux coordinate system (α, β, φ), where α is the toroidal flux, β is the poloidal angle, φ is the toroidal angle:

$$-\boldsymbol{\nabla}\times\boldsymbol{\nabla}\times\boldsymbol{A}+\frac{\mathrm{i}\omega}{c^2}\overleftrightarrow{\epsilon}\cdot\boldsymbol{\nabla}\phi+\frac{\omega^2}{c^2}\overleftrightarrow{\epsilon}\cdot\boldsymbol{A}=-\mu_0\boldsymbol{j}_{\mathrm{ext}}$$

$$\mathrm{i}\omega\boldsymbol{\nabla}\cdot\overleftrightarrow{\epsilon}\cdot\boldsymbol{\nabla}\phi+\omega^2\boldsymbol{\nabla}\cdot\overleftrightarrow{\epsilon}\cdot\boldsymbol{A}=-\frac{1}{\epsilon_0}\boldsymbol{\nabla}\cdot\boldsymbol{j}_{\mathrm{ext}}.$$

In the code, finite difference method is used in the α direction, and the Fourier decomposition in the β and φ directions. We obtain an eigen function, eigen frequency, and decay or growth rate by searching for the complex frequency ω which makes the volume-averaged wave electric field maximum and sufficiently large for given external current $\boldsymbol{j}_{\mathrm{ext}}$ proportional to the electron density[1]. Though it seems possible, at least analytically, to find eigen functions by minimizing the determinant of the coefficient matrix in the finite difference equation, we could not find valid solutions for realistic configurations by this method.

Derivation of Multi-Fluid Conductivity Tensor

We introduce local orthogonal coordinates (x, y, z) for simplicity to derive the conductivity tensors. Here, $\hat{z}=\boldsymbol{B}_0/B_0$, $\hat{x}=\boldsymbol{\nabla}\alpha/|\boldsymbol{\nabla}\alpha|$, and $\hat{y}=\hat{z}\times\hat{x}$. We derive a conductivity tensor by linearizing the multi-fluid equations

$$\frac{\partial n_j}{\partial t}+\boldsymbol{\nabla}\cdot(n_j\boldsymbol{u}_j)=0,\qquad \frac{d}{dt}\left(P_j n_j^{-\gamma}\right)=0$$

$$m_j n_j\left(\frac{\partial}{\partial t}+\boldsymbol{u}_j\cdot\boldsymbol{\nabla}\right)\boldsymbol{u}_j=-\boldsymbol{\nabla}P_j+e_j n_j\left(\boldsymbol{E}+\boldsymbol{u}_j\times\boldsymbol{B}\right)-\sum_{k\neq j}n_j m_j n_k\langle\sigma v\rangle_{jk}(\boldsymbol{u}_j-\boldsymbol{u}_k)$$

where $\langle\sigma v\rangle_{jk}$ is the collision rate between the particle species j and k. Other notations are standard. For a one-ion species plasma, we have the conductivity tensor $\overleftrightarrow{\sigma}_{j,xyz}$ in the orthogonal coordinates,

$$\begin{pmatrix} \overleftrightarrow{I} & \overleftrightarrow{X}_{ie} \\ \overleftrightarrow{X}_{ei} & \overleftrightarrow{I} \end{pmatrix} \begin{pmatrix} \overleftrightarrow{\sigma}_{i,xyz} \\ \overleftrightarrow{\sigma}_{e,xyz} \end{pmatrix} = \begin{pmatrix} \overleftrightarrow{\sigma}_{0i} \\ \overleftrightarrow{\sigma}_{0e} \end{pmatrix}$$

$$\overleftrightarrow{\sigma}_{0j} = \frac{\mathrm{i}e_j^2 n_{j0}}{m_j} \overleftrightarrow{C}_j \cdot \left(\overleftrightarrow{I} + \frac{1}{\omega} \boldsymbol{u}_{j0} \times \boldsymbol{k} \times \right), \qquad \overleftrightarrow{X}_{jk} = -\mathrm{i}n_{j0} \frac{e_k}{e_j} \overleftrightarrow{C}_j \cdot \left(\overleftrightarrow{I} - \frac{\boldsymbol{u}_{j0}\boldsymbol{k}}{\omega} \right) \langle\sigma v\rangle_{jk}$$

$$\overleftrightarrow{C}_j = \frac{\overleftrightarrow{M}_j}{(\omega'_j + \mathrm{i}\nu_j)} \cdot \left[\overleftrightarrow{I} + \frac{\gamma T_j}{m_j \omega W_j} \boldsymbol{k}'_j \boldsymbol{k} \cdot \overleftrightarrow{M}_j \right], \qquad W_j = \omega'_j + \mathrm{i}\nu_j - \frac{\gamma T_j}{m_j \omega} \boldsymbol{k} \cdot \overleftrightarrow{M}_j \cdot \boldsymbol{k}'_j$$

$$\overleftrightarrow{M}_j = \delta^{-1} \times \begin{pmatrix} (\omega'_j + \mathrm{i}\nu_j)^2 & \mathrm{i}\Omega_j(\omega'_j + \mathrm{i}\nu_j) & 0 \\ -\mathrm{i}(\Omega_j + u'_{j0y} - Z_j k_y)(\omega'_j + \mathrm{i}\nu_j) & (\omega'_j + \mathrm{i}\nu_j)(\omega'_j + \mathrm{i}\nu_j - \mathrm{i}Z_j k_x) & 0 \\ -\mathrm{i}(u'_{j0z} - Z_j k_z)(\omega'_j + \mathrm{i}\nu_j) & \Omega_j(u'_{j0z} - Z_j k_z) & \delta \end{pmatrix}$$

$$\delta = (\omega'_j + \mathrm{i}\nu_j)(\omega'_j + \mathrm{i}\nu_j - \mathrm{i}Z_j k_x) - \Omega_j(\Omega_j + u'_{j0y} - Z_j k_y)$$

$$Z_j = \frac{1}{m_j n_{j0} \omega'_j} \left(\gamma T_{j0} \frac{dn_{j0}}{dx} - \frac{dP_{j0}}{dx} \right), \qquad \nu_j = \sum_{k \neq j} n_{k0} \langle\sigma v\rangle_{jk}$$

where, $\omega'_j = \omega - \boldsymbol{k}\cdot\boldsymbol{u}_{j0}$, $\gamma T_j \boldsymbol{k}'_j = \gamma T_j \boldsymbol{k} + \omega'_j m_j \boldsymbol{u}_{j0} + \mathrm{i}e_j \boldsymbol{E}_0 + \mathrm{i}m_j \sum_{k\neq j} \langle\sigma v\rangle_{jk} n_{k0} \boldsymbol{u}_{k0}$, $\Omega_j = e_j B_0 / m_j$, $u'_{j0i} \equiv du_{j0i}/dx$.

Results of Numerical Calculation

We show preliminary results of the numerical analysis for internal kink mode, external kink mode, and resistive wall mode. Fig.1 shows the growth rates of the internal kink mode calculated by TASK/WA (solid line) and the formula obtained by Martynov et al[3] (broken line):

$$\gamma\tau_A = 0.5\epsilon_1(\kappa_1 - 0.5)\left(\beta_{bu} - \left(0.5 - \frac{\epsilon_1}{\epsilon_a}(\kappa_1 - 1.5|\delta_1 + 0.04|) \right) \right)^{(1.23-1.26\epsilon_1)} \tag{1}$$

where τ_A is the Alfvén time, $\beta_{bu} = 2\mu_0(\langle p\rangle_1 - p_1)/B_{pl}^2$ is the so-called beta Bussac, $\langle p\rangle_1$ is the volume-averaged pressure inside of the $q = 1$ surface, and p_1, B_{pl}, ϵ_1, κ_1, δ_1 are the pressure, poloidal magnetic field, inverse aspect ratio, elongation, and triangularity on $q = 1$ surface, respectively. ϵ_a is the inverse aspect ratio on the plasma edge. The eigen function for $\beta_{bu} = 0.303$ is shown in Fig.2. In the present calculations, $\epsilon_1 = 0.12$, $\epsilon_a = 0.33$, $\kappa_1 = 1$, and $\delta_1 = 0$. Though the gradient of the growth rates obtained by TASK/WA agrees with Eq. (1), $\gamma\tau_A$ shifts upward by about 0.017 for a wide rage of β_{bu}. This discrepancy may be attributed to other destabilizing mechanism such as parallel current, but not yet understood well. Fig.3 shows growth rates of the external kink mode for a plasma with flat pressure profile, flat q profile in the plasma, and large aspect ratio ($R_0 = 20$m). This result agrees well with the analytic solutions for a cylindrical plasma. Fig.4 shows the growth rates of 2/1 external kink

mode as a function of perfectly conducting wall radius (solid line) and the growth rates of resistive wall mode as a function of resistive wall radius (broken line). We see that resistive mode becomes unstable for the wall radius where the external kink mode is stabilized.

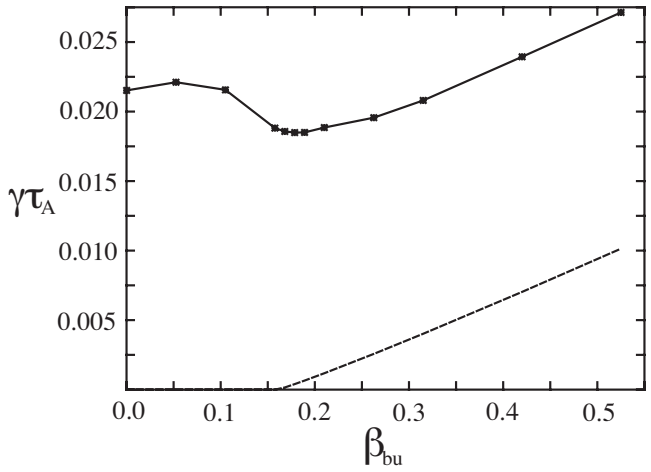

Fig.1: Growth rate of the internal kink mode (n = 1) as a function of β_{bu}. Growth rate obtained by TASK/WA (solid line) and Eq. (1) (dotted line).

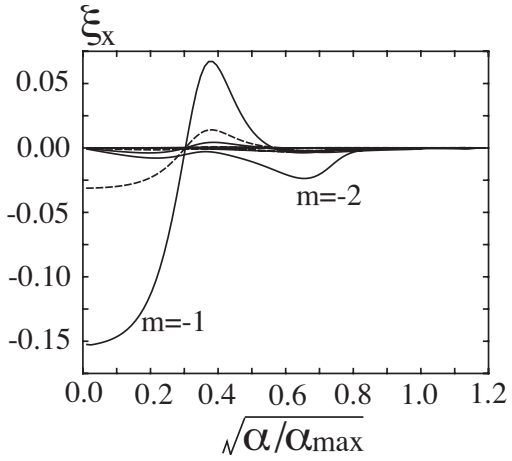

Fig. 2: Eigen function (radial displacement) for internal kink mode (β_{bu} = 0.303)

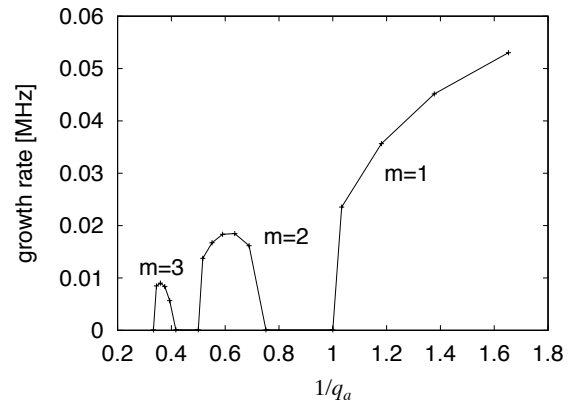

Fig.3: Growth rate of the external kink mode (n = 1) for a large aspect ratio, flat pressure profile, and flat q-profile plasma.

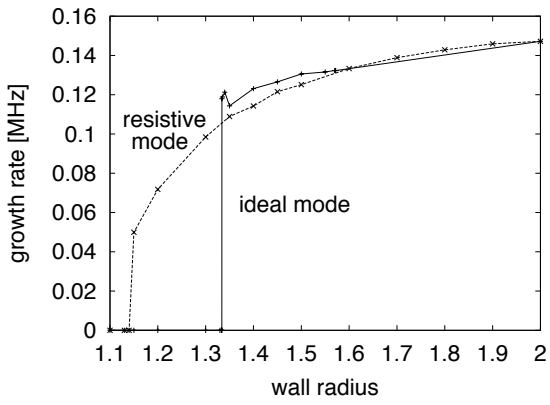

Fig.4: Growth rate of the external kink mode (solid line) and the resistive wall mode (dotted line) as functions of perfectly conducting (resistive) wall radius (q_a = 1.731)

Derivation of Kinetic Dielectric Tensor

The derivation of a kinetic dielectric tensor starts from introducing action variable $\boldsymbol{J}$ and angle variable $\boldsymbol{\Theta}$ of a particle[2], where $\boldsymbol{J} \equiv (m_j\mu/e_j, p_\varphi, J_P)$, μ is the magnetic moment, p_φ is the canonical angular momentum in the toroidal direction, J_P is the toroidal flux surrounded by a drift orbit; the generalized coordinates conjugate to $\boldsymbol{J}$ are denoted by $\boldsymbol{\Theta} \equiv (\Theta_g, \Phi, \Theta_P)$. Once particle orbit is expressed as a function of the action and angle variables, the perturbed

distribution function can be integrated along the orbits to obtain the perturbed current

$$\boldsymbol{j}(\boldsymbol{x}) = (2\pi)^3 \int d^3x' \int d^3J \sum_{\boldsymbol{l}} \frac{\boldsymbol{l}}{\boldsymbol{l}\cdot\boldsymbol{\omega}(\boldsymbol{J}) - \omega} \cdot \frac{\partial f_0(\boldsymbol{J})}{\partial \boldsymbol{J}} \times \{-\boldsymbol{j}_{\boldsymbol{l}}^*(\boldsymbol{x}|\boldsymbol{J})\boldsymbol{j}_{\boldsymbol{l}}(\boldsymbol{x}'|\boldsymbol{J})\cdot\boldsymbol{A}(\boldsymbol{x}') + \boldsymbol{j}_{\boldsymbol{l}}^*(\boldsymbol{x}|\boldsymbol{J})\rho_{\boldsymbol{l}}(\boldsymbol{x}'|\boldsymbol{J})\phi(\boldsymbol{x}')\}, \quad (2)$$

where $\boldsymbol{\omega} = d\boldsymbol{\Theta}/dt$, $\boldsymbol{l} \equiv (l_g, l_\varphi, l_P)$ is the wave number vector, f_0 is the unperturbed distribution function, and

$$\boldsymbol{j}_{\boldsymbol{l}}(\boldsymbol{x}'|\boldsymbol{J}) = \frac{1}{(2\pi)^3} \oint e_j \boldsymbol{v}(\boldsymbol{J},\boldsymbol{\Theta})\delta(\boldsymbol{x}' - \boldsymbol{r}(\boldsymbol{J},\boldsymbol{\Theta}))\exp(-\mathrm{i}\boldsymbol{l}\cdot\boldsymbol{\Theta})\, d^3\Theta,$$

$$\rho_{\boldsymbol{l}}(\boldsymbol{x}'|\boldsymbol{J}) = \frac{1}{(2\pi)^3} \oint e_j \delta(\boldsymbol{x}' - \boldsymbol{r}(\boldsymbol{J},\boldsymbol{\Theta}))\exp(-\mathrm{i}\boldsymbol{l}\cdot\boldsymbol{\Theta})\, d^3\Theta.$$

In order to integrate Eq.(2) with respect to $\boldsymbol{x}'$, we apply the Fourier series expansion for $\boldsymbol{A}(\boldsymbol{x}'(\boldsymbol{J},\boldsymbol{\Theta}))$ and $\phi(\boldsymbol{x}'(\boldsymbol{J},\boldsymbol{\Theta}))$ expand them into power series around a guiding center position $(\alpha_{gc}, \beta_{gc}, \varphi_{gc})$ with respect to the larmor radius ρ, and integrate Eq.(2) with respect to Θ_g and Φ. Finally we have

$$\boldsymbol{j}_{kmn}(\boldsymbol{x}) = \frac{1}{2\pi} \int d^3J \sum_{\boldsymbol{l}} \frac{\boldsymbol{l}}{\boldsymbol{l}\cdot\boldsymbol{\omega} - \omega} \cdot \frac{\partial f_0}{\partial \boldsymbol{J}}(\boldsymbol{J})\boldsymbol{j}_{\boldsymbol{l}}^*(\boldsymbol{x}|\boldsymbol{J})\, e_j \times \int d\Theta_P\, e^{\mathrm{i}(-l_P\Theta_P + k\alpha_{gc} + m\beta_{gc} + n\tilde{\varphi}_{gc})} \times \left[-\left\{\boldsymbol{v}_{gc}J_0(k_\perp\rho) + \mathrm{i}v_{\mathrm{larmor}}(\hat{\boldsymbol{k}}_\perp \times \boldsymbol{b})J_1(k_\perp\rho)\right\}\boldsymbol{A}_{kmn} + \phi_{kmn}J_0(k_\perp\rho)\right].$$

where J_0 and J_1 are the Bessel functions, $\tilde{\varphi}_{gc} = \varphi_{gc} - \Phi$, $v_{\mathrm{larmor}} = \sqrt{2\mu B_0/m_j}$, $\boldsymbol{v}_{gc} = (\dot{\alpha}_{gc}, \dot{\beta}_{gc}, \dot{\varphi}_{gc})$, and $\boldsymbol{v}_{gc}$ satisfies the following equations.

$$\dot{\beta} = \frac{1}{e_j}\frac{\partial H_0}{\partial \alpha}, \qquad e_j\dot{\alpha} = -\frac{\partial H_0}{\partial \beta}, \qquad \dot{\varphi} = \frac{p_\varphi - e_j\psi_p(\alpha)}{m_j\mathcal{R}^2}$$

$$H_0 = \frac{1}{2m_j\mathcal{R}^2}\left[p_\varphi - e_j\psi_p(\alpha)\right]^2 + \mu B_0 + e_j\phi_0, \qquad \mathcal{R} = \frac{B_0 R}{B_\varphi}$$

Numerical simulation using this kinetic dielectric tensor is left for further study.

References

[1] A. Fukuyama and T. Akutsu, Kinetic Global Analysis of Alfvén Eigenmodes in Toroidal Plasmas, Proc. of IAEA Fusion Energy Conference (Lyon, France) IAEA-CN-94/TH/P3-14

[2] A. N. Kaufman, Phys. Fluids **15** 1063 (1972)

[3] An. Martynov, O. Sauter, Shape and Aspect Ratio Effects on the Ideal Internal Kink Mode, Proc. Joint Varenna-Lausanne Int. Workshop (Varenna 2002) 297